

Supporting information for

Achieving efficient Tb³⁺ dual-mode luminescence via the Gd-sublattice-mediated energy migration in NaGdF₄ core-shell nanoarchitecture

Mingye Ding,^a Daqin Chen,^{a*} Zongyi Wan,^a Yang Zhou,^a Jiasong Zhong,^a Junhua Xi,^a Zhenguo Ji^a

^a College of Materials & Environmental Engineering, Hangzhou Dianzi University, Hangzhou, 310018, P. R. China

E-mail: dqchen@hdu.edu.cn (D. Chen)

Experimental section

Reagents. All of the chemical reagents used in this experiment are analytical grade and were received without further purification. GdCl₃·6H₂O (99.99%), YbCl₃·6H₂O (99.99%), TmCl₃·6H₂O (99.995%), CeCl₃·6H₂O (99.99%) and TbCl₃·6H₂O (99.99%) were purchased from Beijing Founde Star Science & Technology Co., Ltd. NaOH (98%), NH₄F (98%), methanol (99.5%), and ethanol (99.7%) were provided by Sinopharm Chemical Reagent Co., Ltd. Oleic acid (OA, 90%), 1-octadecene (ODE, 90%) were received from Aladdin Reagent Company.

Synthesis of NaGdF₄:Yb/Tm core nanoparticles. In a typical experiment, GdCl₃·6H₂O (0.5576g, 1.5 mmol), YbCl₃·6H₂O (0.5697g, 1.47 mmol), TmCl₃·6H₂O (0.0115g, 0.03 mmol) were taken in a 100 mL 3-necked flask at room temperature, and 30 mL of ODE along with 30 mL of OA was added. The resulting mixture was then heated to 160 °C under a N₂ atmosphere and held at this temperature for 15 min to get a homogeneous solution. Subsequently, the flask was cooled down to 60 °C, and 20 mL methanol solution containing NH₄F (0.463 g, 12 mmol), NaOH (0.300 g, 7.5 mmol) was added dropwise and stirred at 60 °C for 30 min to ensure that all fluoride was consumed completely. The reaction temperature was then increased to 100 °C to remove the methanol from the reaction mixture. Upon removal of methanol, the solution was heated to 310 °C and maintained at this temperature under a nitrogen flow for 60 min, at which time the mixture was cooled down to room temperature. The resulting nanoparticles were precipitated out through an addition of ethanol (20 mL), collected by centrifugation at 10000 rpm for 10 min, washed with ethanol three times, and finally dried at 60 °C in vacuum for 12 h.

Synthesis of NaGdF₄:Yb/Tm@NaGdF₄:Ce/Tb core-shell nanoparticles. For synthesis of

core/shell structure, $\text{GdCl}_3 \cdot 6\text{H}_2\text{O}$ (0.2732 g, 0.735 mmol), $\text{CeCl}_3 \cdot 6\text{H}_2\text{O}$ (0.0587g, 0.1575 mmol), and $\text{TbCl}_3 \cdot 6\text{H}_2\text{O}$ (0.0588g, 0.1575 mmol) were added to the mixture of 6 mL OA and 15 mL ODE in a three-necked flask (100 mL) at room temperature. Then, the slurry was heated to 160 °C under a N_2 atmosphere with vigorous magnetic stirring for 15 min to form an optically transparent solution. After the mixture was cooled down to 60 °C, the as-prepared core nanoparticles (0.2124 g) in 4 mL cyclohexane were added along with a 10 mL methanol solution of NH_4F (0.170 g, 4.4 mmol) and NaOH (0.0115 g, 2.75 mmol). The resulting mixture was stirred at 60 °C for 30 min, at which time the reaction temperature was increased to 100 °C to remove the cyclohexane and methanol. Then the solution was heated at 310 °C under a nitrogen flow for 60 min and cooled down to room temperature. The resulting core-shell nanoparticles were precipitated out by the addition of ethanol, collected by centrifugation, washed with ethanol three times and finally dried at 60 °C in vacuum for 12 h.

Characterization. Powder X-ray diffraction (XRD) measurements were performed on an AXS D8 advance diffractometer at a scanning rate of 10 °/min in the 2θ range from 10° to 80° with Cu $\text{K}\alpha$ radiation ($\lambda=0.15406$ nm). Transmission electron microscopy (TEM) and selected area electron diffraction (SAED) patterns were recorded on JEM-200CX with a field emission gun operating at 200 kV. Images were acquired digitally on a Gatan multiple CCD camera. UC emission spectra were recorded with a Jobinyvon FL3-221 fluorescence spectrophotometer equipped with a 980 nm laser diode Module (K98SA3M-54W, China) as the excitation source. All the measurements were performed at room temperature.

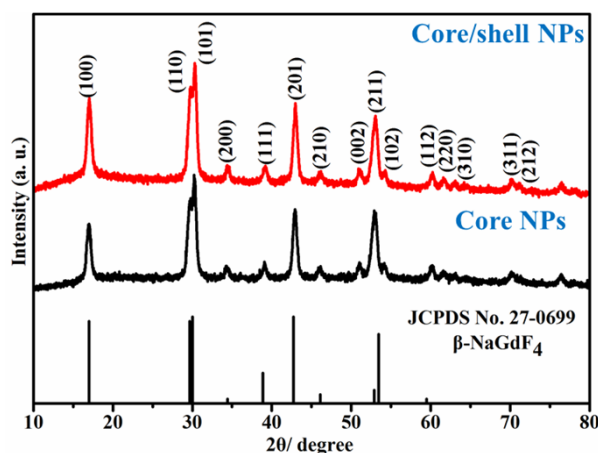


Fig. S1 The XRD patterns for $\text{NaGdF}_4:49\%\text{Yb}^{3+}/1\%\text{Tm}^{3+}$ core NPs, and $\text{NaGdF}_4:49\%\text{Yb}^{3+}/1\%\text{Tm}^{3+}@\text{NaGdF}_4:15\%\text{Ce}^{3+}/15\%\text{Tb}^{3+}$ core-shell NPs. The standard data for hexagonal NaGdF_4 (JCPDS No. 27-0699) is shown as a reference.

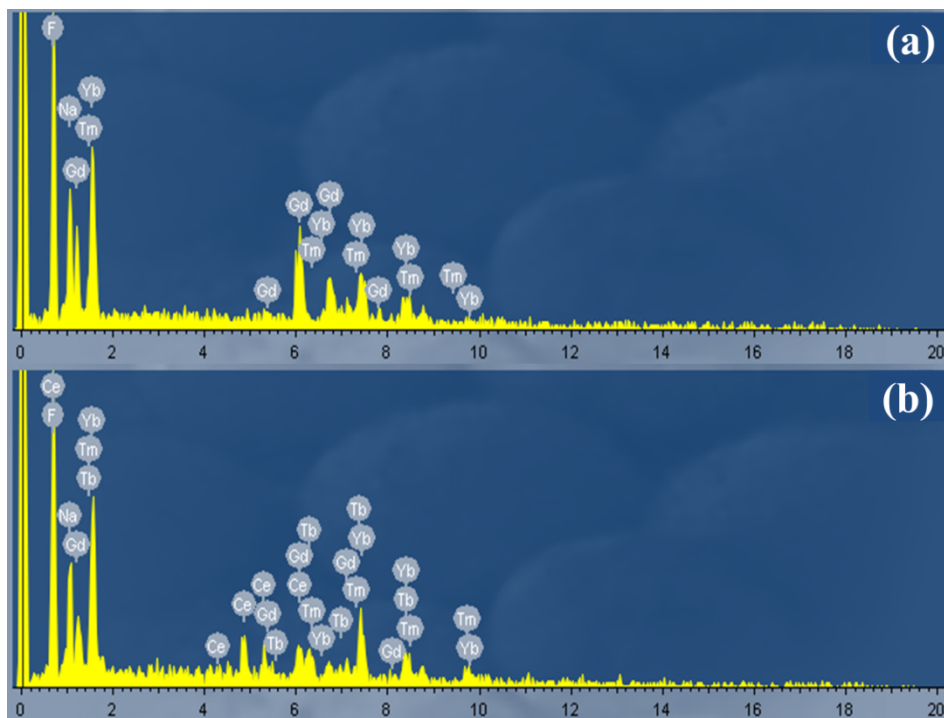


Fig. S2 The energy-dispersive X-ray spectroscopy analyses of (a) $\text{NaGdF}_4:\text{Yb}^{3+}/\text{Tm}^{3+}$ core NPs and (b) $\text{NaGdF}_4:\text{Yb}^{3+}/\text{Tm}^{3+}@\text{NaGdF}_4:\text{Ce}^{3+}/\text{Tb}^{3+}$ core-shell NPs, revealing the presence of the doped elements of Yb, Tm for core NPs and Yb, Tm, Ce and Tb for core-shell NPs.

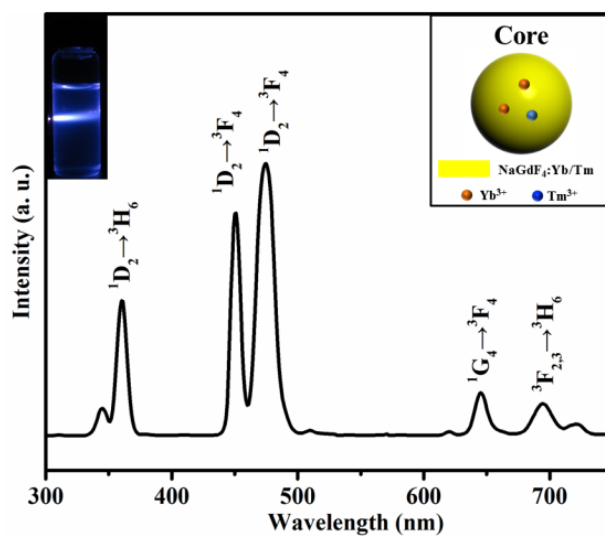


Fig. S3 UC emission of $\text{NaGdF}_4:49\%\text{Yb}^{3+}/1\%\text{Tm}^{3+}$ core NPs under the excitation of a 980 nm continuous wave (CW) diode laser at a power density of $10 \text{ W}/\text{cm}^2$. The emission spectra were obtained in cyclohexane solutions comprising 1 wt% NPs under 980 nm laser diode excitation.

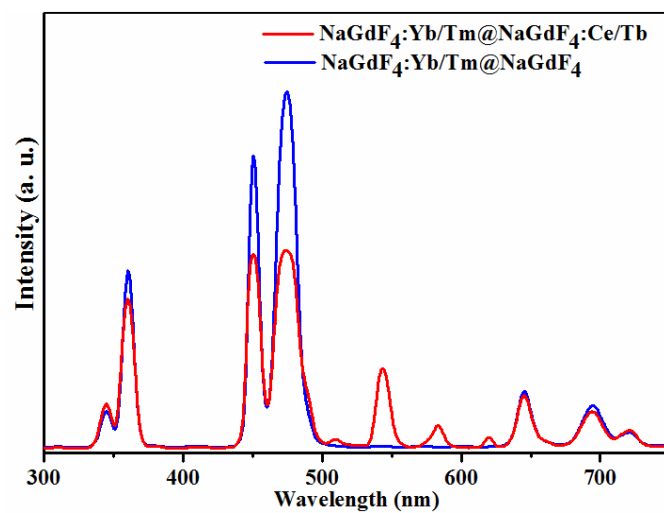


Fig. S4 UC emission spectra of $\text{NaGdF}_4\text{:}49\%\text{Yb}^{3+}/1\%\text{Tm}^{3+}@\text{NaGdF}_4\text{:}15\%\text{Ce}^{3+}/15\%\text{Tb}^{3+}$ and $\text{NaGdF}_4\text{:}49\%\text{Yb}^{3+}/1\%\text{Tm}^{3+}@\text{NaGdF}_4$ core-shell NPs.

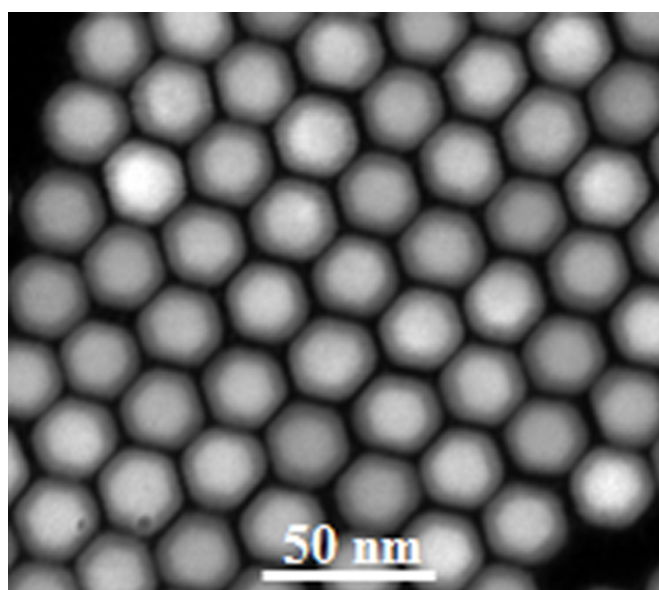


Fig. S5 STEM-HADDF image of $\text{NaGdF}_4\text{:Yb}^{3+}/\text{Tm}^{3+}@\text{NaYF}_4\text{:Ce}^{3+}/\text{Tb}^{3+}$ core-shell nanoparticles.

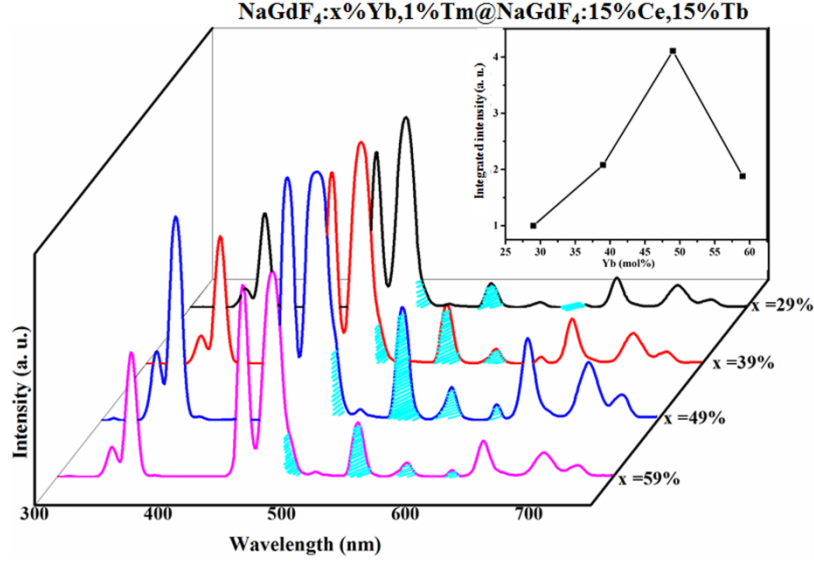


Fig. S6 EMU emission spectra for a series of NaGdF₄:x%Yb³⁺/1%Tm³⁺@NaGdF₄:15%Ce³⁺/15%Tb³⁺ core-shell NPs as a function of different dopant concentrations of Yb³⁺ ions (x = 29, 39, 49, 59). The emission spectra were obtained in cyclohexane solutions comprising 1 wt% NPs under 980 nm laser diode excitation.

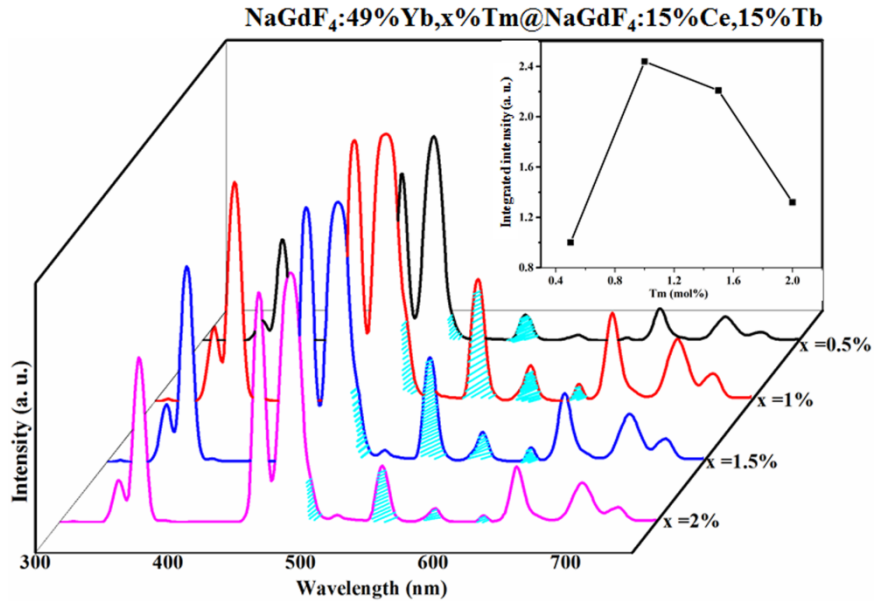


Fig. S7 EMU emission spectra for a series of NaGdF₄:49%Yb³⁺/x%Tm³⁺@NaGdF₄:15%Ce³⁺/15%Tb³⁺ core-shell NPs as a function of different dopant concentrations of Tm³⁺ (x=0.5, 1, 1.5, 2). The emission spectra were obtained in cyclohexane solutions comprising 1 wt% NPs under 980 nm laser diode excitation.

As we known, the dopant concentration of lanthanide ions has a great impact on luminescence properties via tuning the average distance between neighboring dopant ions^{1, 2}. Thus, a series of NaGdF₄:Yb³⁺/Tm³⁺@NaGdF₄:Ce³⁺/Tm³⁺ core-shell NPs were synthesized in order to optimize doping concentration of the Yb³⁺/Tm³⁺ ion pair for efficient EMU process. In our experiments, the core was doped with various concentrations of Yb³⁺ and Tm³⁺ ions, while the dopant concentrations

of Tb^{3+} and Ce^{3+} in the shell were fixed to be 15 and 15 mol%, respectively. By comparing the emission intensity of Tb^{3+} , we found that the optimum dopant concentration of Yb^{3+} and Tm^{3+} for achieving maximum Tb^{3+} emission were 49, 1 mol%, respectively (Fig. S6 and Fig. S7). To optimize dopant concentrations of Ce^{3+} and Tb^{3+} ions for achieving efficient DC process, we also synthesized a series of $\text{NaGdF}_4:\text{Yb}^{3+}/\text{Tm}^{3+}@\text{NaGdF}_4:\text{Ce}^{3+}/\text{Tb}^{3+}$ core-shell NPs with different dopant concentrations of Ce^{3+} and Tb^{3+} in shell layer. From the photoluminescence data of the as-synthesized samples, the optimum concentrations of Ce^{3+} and Tb^{3+} for efficient DC emission under 254 nm excitation is estimated to be 15 and 15 mol%, respectively (Fig. S10 and Fig S11).

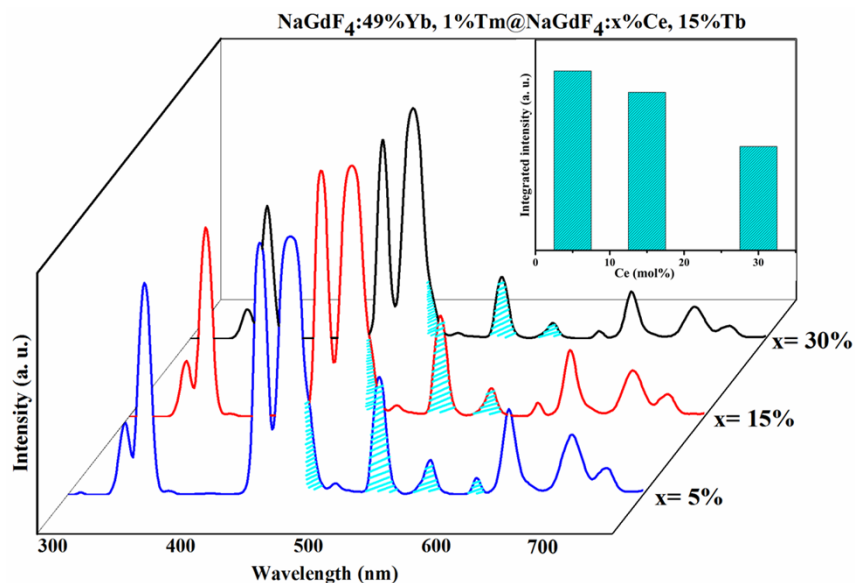


Fig. S8 EMU emission spectra for a series of $\text{NaGdF}_4:49\%\text{Yb}^{3+}/1\%\text{Tm}^{3+}@\text{NaGdF}_4:x\%\text{Ce}^{3+}/15\%\text{Tb}^{3+}$ core-shell NPs as a function of different dopant concentrations of Ce^{3+} (5-30 mol%).

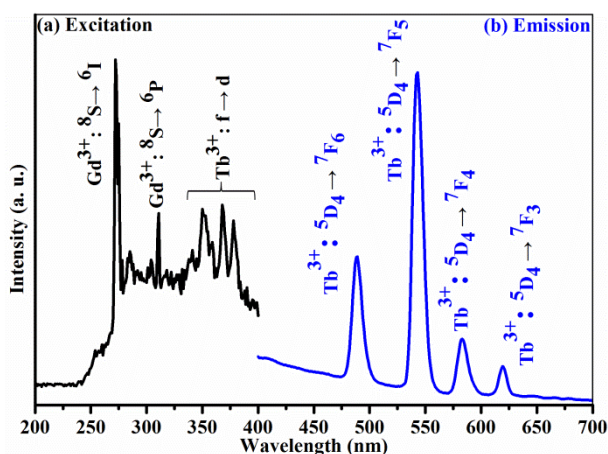


Fig. S9 (a) PL excitation ($\lambda_{\text{em}} = 543 \text{ nm}$) and (b) DC emission ($\lambda_{\text{ex}} = 275 \text{ nm}$) spectra for Tb^{3+} in $\text{NaGdF}_4:\text{Yb}^{3+}/\text{Tm}^{3+}@\text{NaYF}_4:\text{Tb}^{3+}$ core-shell NPs.

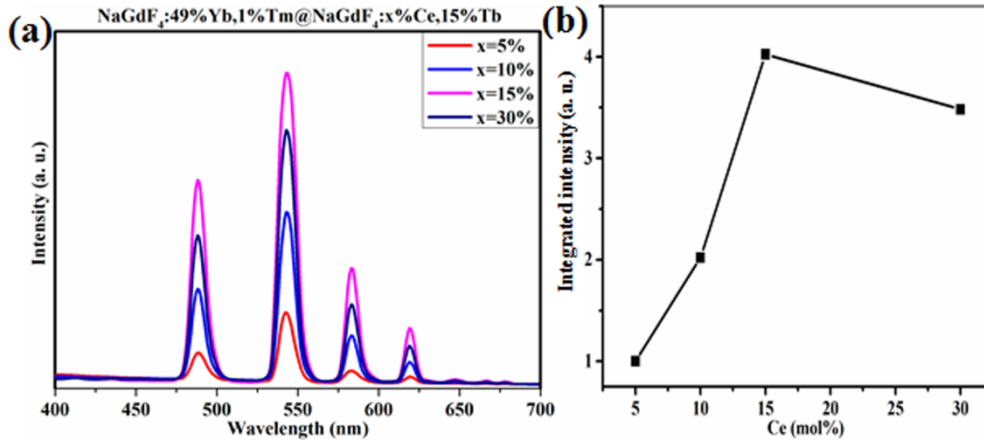


Fig. S10 DC emission spectra ($\lambda_{\text{ex}} = 254 \text{ nm}$) for the as-obtained NaGdF₄:49%Yb³⁺/1%Tm³⁺@NaGdF₄:x%Ce³⁺/15%Tb³⁺ core-shell NPs as a function of different dopant concentrations of Ce³⁺ (5-30 mol%).

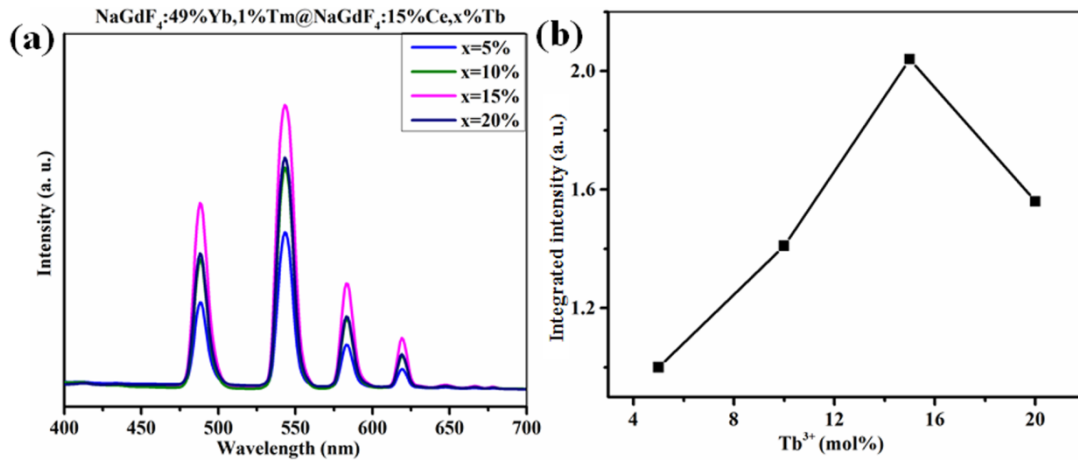


Fig. S11 DC emission spectra ($\lambda_{\text{ex}} = 254 \text{ nm}$) for the as-obtained NaGdF₄:49%Yb³⁺/1%Tm³⁺@NaGdF₄:15%Ce³⁺/x%Tb³⁺ core-shell NPs as a function of different dopant concentrations of Tb³⁺ (5-20 mol%).

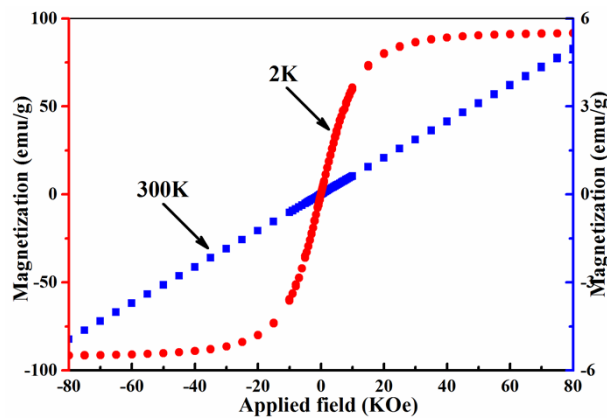


Fig. S12 Magnetization as a function of applied field for NaGdF₄:Yb³⁺/Tm³⁺@NaGdF₄:Ce³⁺/Tb³⁺ core-shell NPs at 2 K and 300K.

Apart from efficient UC and DC luminescence, NaGdF₄:Yb/Tm@NaGdF₄:Ce/Tb core-shell NPs also exhibit paramagnetism at room temperature, originating from the intrinsic magnetic moment of Gd³⁺ with non-interacting and localized nature³⁻⁵. As shown in Fig. S12, the

magnetization of the core-shell nanocrystals at 20 KOe is around 1.5 emu/g, which is close to the reported value of the NPs used for common bio-separation. At low temperature (2 K), these core-shell NPs exhibit superparamagnetism with a saturation magnetization value of 90 emu/g. Hopefully, NaGdF₄:Yb/Tm@NaGdF₄:Ce/Tb core-shell NPs with dual-mode luminescence and proper paramagnetism are ideal for bio-labeling and magnetic resonance imaging applications in the further, after appropriate surface modifications.

References

1. F. Wang and X. Liu, *Chem. Soc. Rev.*, 2009, 38, 976-989.
2. F. Wang, R. Deng, J. Wang, Q. Wang, Y. Han, H. Zhu, X. Chen and X. Liu, *Nat. Mater.*, 2011, 10, 968-973.
3. D. Dosev, M. Nickkova, R. K. Dumas, S. J. Gee, B. D. Hammock, K. Liu and I. M. Kennedy, *Nanotechnology*, 2007, 18, 055102.
4. Z. Liu, G. Yi, H. Zhang, J. Ding, Y. Zhang and J. Xue, *Chem. Commun.*, 2008, 6, 694-696.
5. D. Chen, Y. Yu, F. Huang, A. Yang and Y. Wang, *J. Mater. Chem.*, 2011, 21, 6186-6192.